SRNL-STI-2011-00209

Keywords:
DWPF
Canister
Thermal

Retention: *permanent*

COMSOL Multiphysics Model for DWPF Canister Filling

M.R.Kesterson

March 31, 2011

Applied Computational Engineering and Statistics
Savannah River National Laboratory
Aiken, SC 29808

This document was prepared in conjunction with work accomplished under Contract No. DE-AC09-08SR22470 with the U.S. Department of Energy.

SRNL
SAVANNAH RIVER NATIONAL LABORATORY
TM

DISCLAIMER

This document was prepared in conjunction with work accomplished under Contract No. DE-AC09-08SR22470 with the U.S. Department of Energy.

AUTHORS:

M.R, Kesterson, Applied Computational Engineering and Statistics Date
Savannah River National Laboratory

TECHNICAL REVIEWERS:

N.K.Gupta, Applied Computational Engineering and Statistics Date
Savannah River National Laboratory

APPROVERS:

J.W. Amoroso, Customer Date
Process Technology Programs

A.L. Billings, Customer Date
Process Technology Programs

P.L. Lee, Manager Applied Computational Engineering and Statistics Date
Savannah River National Laboratory

Table of Contents

List of Tables

List of Figures

1. Introduction and Background

The purpose of this work was to develop a model that can be used to predict temperatures of the glass in the Defense Waste Processing Facility (DWPF) canisters during filling and cooldown. Past attempts to model these processes resulted in large (>200K) differences in predicted temperatures compared to experimentally measured temperatures. This work was therefore intended to also generate a model capable of reproducing the experimentally measured trends of the glass/canister temperature during filling and subsequent cooldown of DWPF canisters.

To accomplish this, a simplified model was created using the finite element modeling software COMSOL Multiphysics [1] which accepts user defined constants or expressions to describe material properties. The model results were compared to existing experimental data [2] for validation.

This work was funded by the Department of Energy (DOE) Office of Environmental Management (EM) technology development task EM-31 WP-5.1.2.

2. Model Description

A simplified model for the DWPF canister and interior space consisting of 13,712 elements was created in Comsol Multiphysics and is shown in Figure 1. The model did not incorporate convective heat transfer ordinarily modeled using Navier-Stokes equations for fluid flow. Rather, a model was developed that incorporated heat transfer by conduction, with the radiation and convection terms approximated by a generalized heat loss function during the canister filling cycle. The reason for developing this type of model was two-fold; 1) the model used a relatively long duration (3000 minutes) timeframe that coupled with the complex nature of the Navier-Stokes equations would extend the computation times to impractical limits and, 2) the convective heat transfer occurring in the glass during pouring was considered minimal below the glass transition temperature.

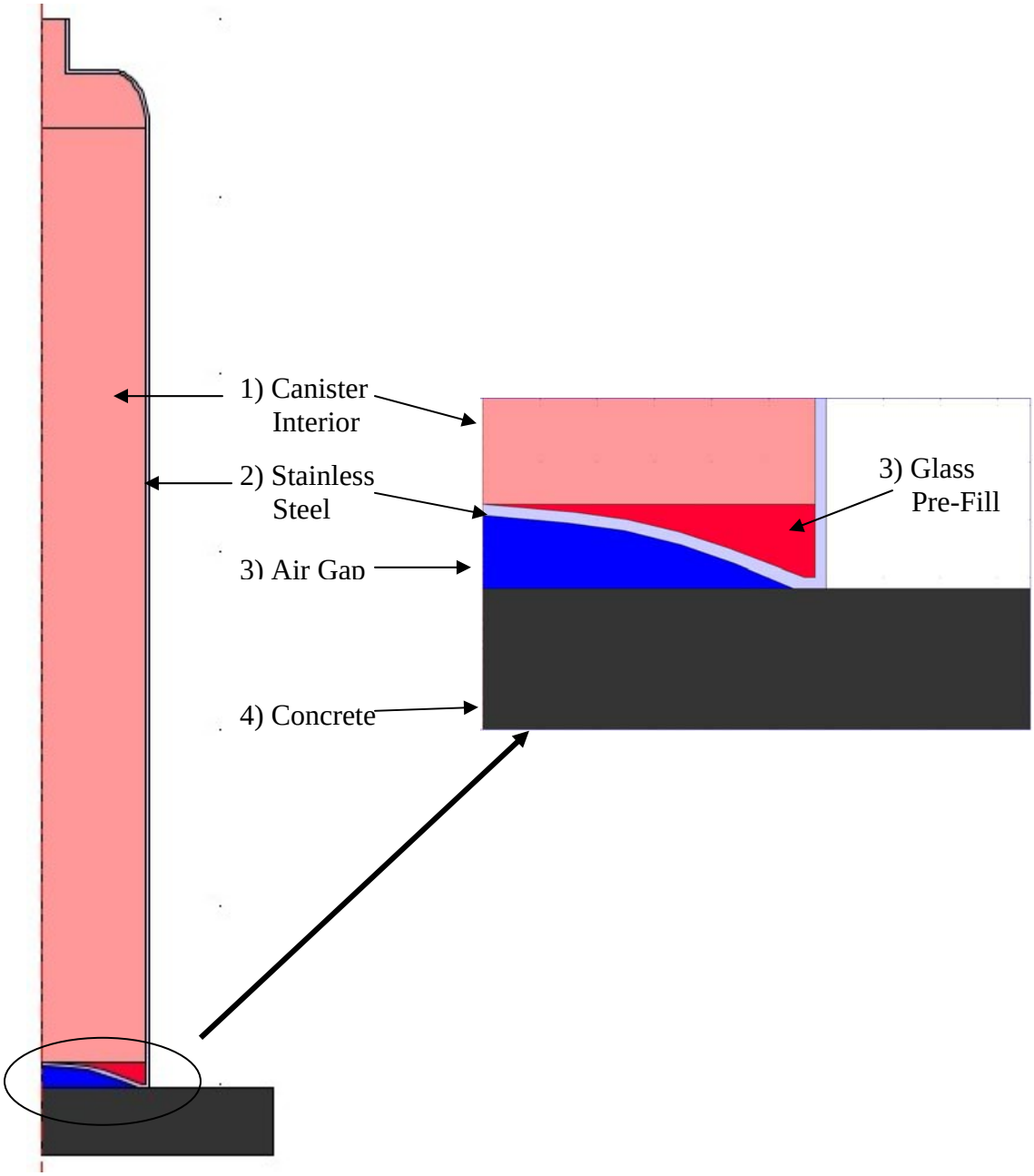

Figure 1 - COMSOL Multiphysics model of the DWPF canister.

For initial stabilization of the simulations, the model contained a small region pre-filled with glass with a volume equivalent to the first 10 minutes of pouring. The region is initialized to the thermal properties of the glass with an initial temperature of 200ºC. This region added a buffer to the sudden transition from air to glass and the resultant change in thermal mass within the canister.

The model incorporated convective heat transfer on the outer surface of the canister as well as radiative losses to ambient. Internally, the walls of the canister exchanged with the glass via radiative heat transfer from the surface of the glass.

In order to model convection and radiative losses from the glass surface, a parameter called Q_loss was employed. Q_loss was designed to encompass to cumulative effect of the radiation losses at the surface along with convection losses below the top surface of the glass:

$$Q\_loss = Q_{radiation} + Q_{convection} \quad [1]$$

The Q_loss parameter employed in the model was a function of the fluid height and varied with radial position:

$$Q\_loss = Q\_loss\_base*(f(z)*f(r)) \quad [2]$$

where Q_loss_base is a constant. In order to obtain these functions based on height and radial distance, the temperature as a function of height was plotted for the initial cooldown period for each thermocouple location. A general quadratic term was fit to the data and written into the COMSOL model. The model was run and the coefficients to the fit were modified until a good fit between the simulation output and the experimental data was achieved. For the Q_loss function, it was found that a quadratic equation coupled with an exponential decrease based on radial position, reasonably approximated the experimental data. The final form of the equation is shown in Appendix A – Global Expressions table.

3. Inputs and Assumptions

Below are the inputs and assumptions that are used in the COMSOL model. All units reported below are used in the model. The COMSOL model has a base unit system of SI, but the user is allowed to input properties in any units and COMSOL converts them to the base unit system for calculations.

Assumptions:

3.1. The ambient temperature in the room is a constant 26ºC. The experimental data shows that the room temperature had variations between 24ºC and 30ºC [2] with an average room temperature that was approximately 26ºC.

3.2. Radiation and convective heat transfer in the enclosed space between the canister bottom and the ground is accounted for by an increased thermal conductivity term.

3.3. The experimental data used was based on scale glass melter run with a nominal pour rate of 228 lb/hr [2]. In reviewing the experimental data, the actual flow rate varied between 190 and 360 lb/hr. A step function was employed in the model to approximate the flow rate variation and more accurately match the experimental conditions. The function is shown in Appendix A – Global Expressions table

Inputs:
3.4. Glass pour temperature is 1080ºC
3.5. Canister dimensions are supplied on drawing W747391 [3]
3.6. Material Properties – Table 1 and Table 2

Table 1 - Material Properties of Canister

Material	Thermal Conductivity		Density (lbm/ft^3)	Specific Heat	
Stainless Steel Canister [4]	$\frac{BTU}{hr \cdot lb_m \cdot {}^oF}$	Temperature (ºF)	494.429	$\frac{BTU}{lb_m \cdot {}^oF}$	Temperature (F)
	3.9915	-328			
	6.28963	-148		0.120	32
	7.74108	32			
	9.43444	212		0.135	752
	12.5793	932			
	14.9983	1292		0.135	3000
	14.9983	3000			

Table 2 - Material Properties of DWPF glass

Material	Thermal Conductivity		Density		Specific Heat	
Glass [4]	$\frac{BTU}{hr \cdot lb_m \cdot {}^oF}$	Temperature (ºF)	(lb/ft^3)	Temperature (ºF)	$\frac{BTU}{lb_m \cdot {}^oF}$	Temperature (ºF)
					0.204	20
	0.76449	20	172.31	20	0.204	68
					0.24	212
	0.76449	68	171.37	392	0.272	392
					0.295	572
	0.76449	1742	167.31	932	0.312	752
					0.325	932
	1.3741	1832	165.44	112	0.334	1112
					0.342	1292
	2.8063	2012	162.94	1292	0.349	1472
					0.354	1652
	3.5079	2102	160.45	1472	0.356	1740
					0.358	1832
	3.5079	3000	157.95	1652	0.362	2012
					0.363	2102
			151.77	2192	0.365	2192
					0.365	3000

The model consisted of two additional regions requiring material properties. These regions were the floor below the canister and the air initially contained within the canister and the air trapped between the canister and the concrete floor. The floor was modeled as

a concrete slab with a lower temperature boundary condition equal to the ambient air temperature. The material library contained within COMSOL is used to obtain the material properties for both the air and concrete.

4. Methodology

Two types of simulations were conducted 1) a post fill simulation and 2) a full simulation that incorporated both filling and cooldown. The purpose for the post fill simulation was to obtain values for the external heat transfer coefficients, particularly due to radiation effects. For this simulation, the model was initialized with a temperature distribution seen in the experimental data at a time of 1074 minutes, a time that is sufficiently past the end of pour time such that heat/glass addition and flow effects can be ignored. Using this temperature distribution as the starting point, the simulation was run to the final 3000 minutes. In this timeframe, the heat loss from the system is due to convective flow at the surface of the canister and radiative effects. The convection heat transfer at the surface of the canister is modeled by generalized equations based on air properties and temperature of the canister surface and the ambient temperature. In addition to the convection heat transfer, radiative heat transfer occurs from the canister surface. The post fill model holds the view factor for the radiation terms constant and the emissivity value was varied in order to match the simulation output with the experimental data.

Once the external heat transfer terms were refined in the post fill case, the parameters were applied to the full model that incorporates both the filling and cooldown phase of the experiment. The full simulation was run in discrete timesteps, typically 40 second increments. A larger time step, up to 240 seconds, was used for rough estimates yielding temperature deviations of approximately 5% over the smaller timestep. Using a timestep of 80 seconds, the temperature deviation was approximately 1%.

Based on the time of the simulation and the time step, a corresponding volume of glass was added to the system by changing the material properties of the subdomain in the region between the calculated new glass height and the previous glass height (glass_height(t) – glass_height(dt)). The material properties for this region were changed from air to those of the glass, specifically changing the specific heat, density, and thermal conductivity. In making this change, heat was also added to the region, since temperature could not be directly imposed. The amount of heat added to the system was based on the specific heat, volume, and density of the differential volume of glass and the difference between the region's current temperature and the temperature of the glass melt.

The temperature of the glass melt was fit to experimental data. The maximum temperatures reported by the thermocouples were plotted as a function of thermocouple location. The curve fit for this data was used in the COMSOL model to define the temperature of the top surface of the glass as it rises in the canister during glass pouring.

In addition to the heat being added to bring the glass up to the correct temperature, a Q_loss term was used to remove heat from the system. This heat loss removal is dependent on the glass height, and radial position in the canister. The actual form of the equation used for Q_loss is shown in Appendix A – Global Expressions table. The

parameters, namely Q_loss_base and how much heat is removed based on radial position and height were obtained based on trial and error fits to the experimental data.

5. Results

5.1. Post Fill Model

Simulations were run in which the canister was pre-filled with glass to a level of 2.38 m, and a temperature distribution in the glass was set to be equal to that seen in the experimental data for 1074 minutes (approximately 150 minutes after the end of the glass pour cycle). The 1074 minutes temperature profile was chosen as the starting point for the cooldown of the glass without additional heat input during the pour phase. The simulation was then run to the full 3000 minutes corresponding to the last of the experimental data and the results were compared to the experimental values. The emissivity value for radiative heat transfer was modified to achieve good agreement with the experimental data as shown in Figure 2 and Figure 3. The results were obtained using a surface emissivity of 0.8 and an external view factor of 1.0.

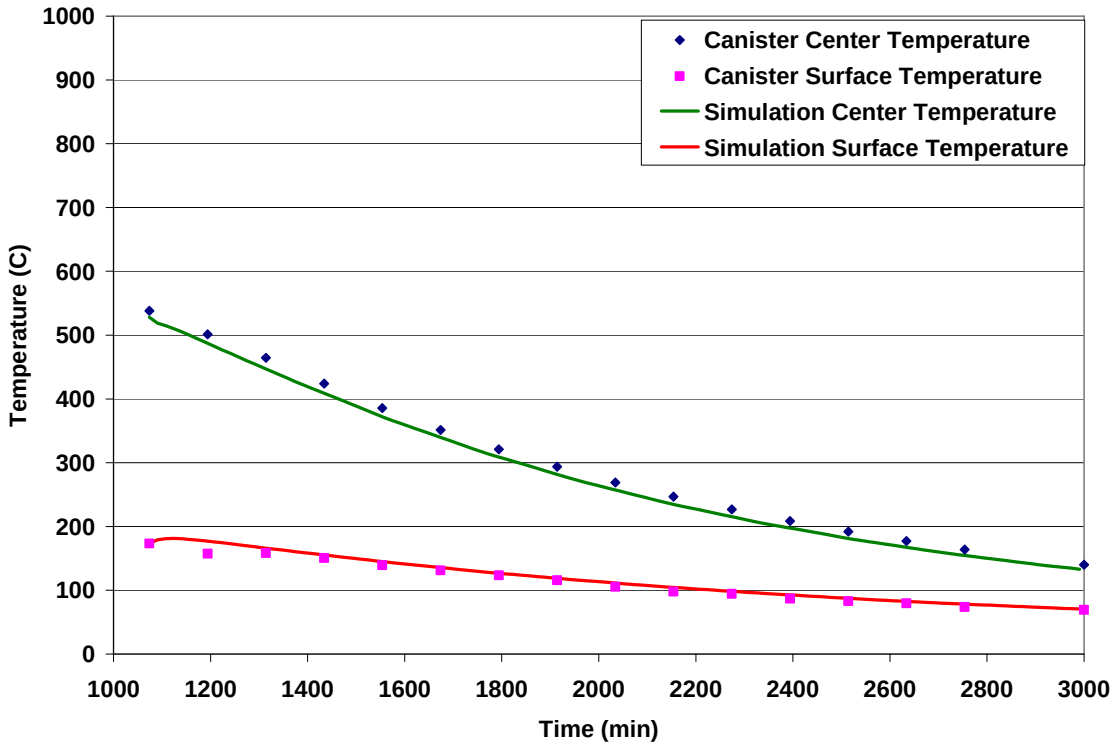

Figure 2 - Temperature profile for 15 inch thermocouple location during the cool down phase.

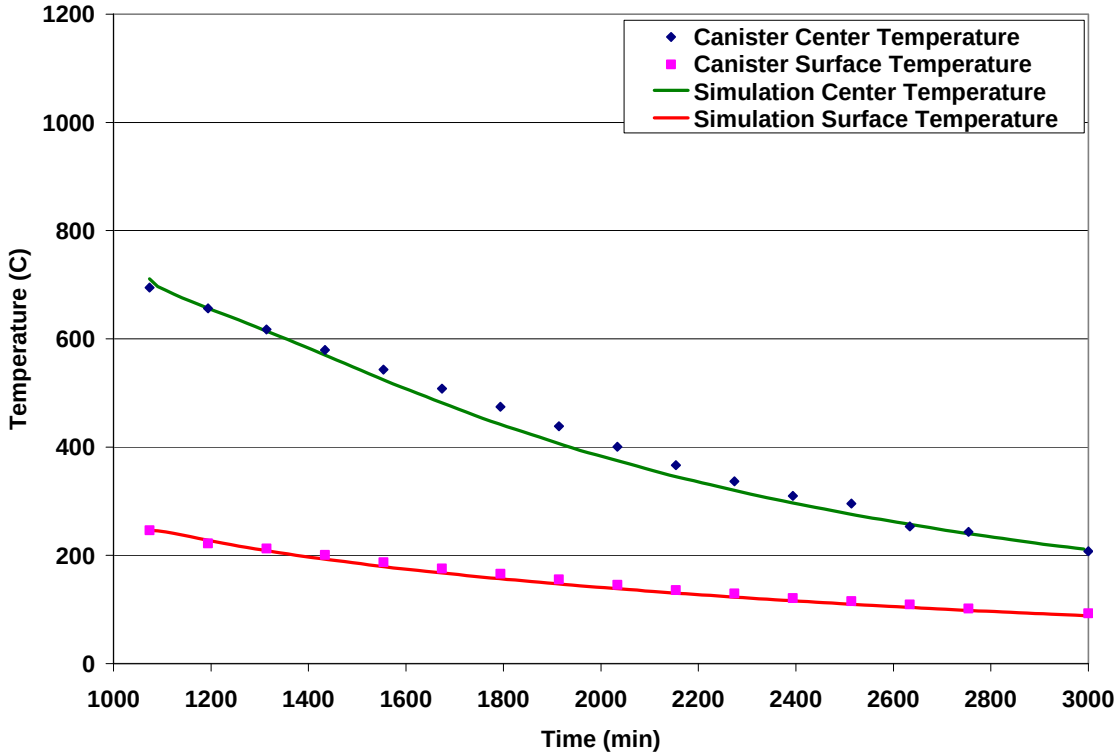

Figure 3 - Temperature profile for 51 inch thermocouple location during the cool down phase.

5.2. Glass Pouring Model

Once the parameters for radiative heat loss for the outside surface of the container were verified, the model was run through an iterative filling process in which the Q_loss term and internal surface radiation terms were varied in order to approximate the temperature profile seen in the experimental data [2].

Figures Figure 4 to Figure 8 show the final results obtained from the model at five thermocouple locations: 1) bottom surface of the canister, 2) 15 inches, 3) 51 inches, 4) 87 inches, and 5) 99 inches. The larger temperature differences predicted at the 99 inch height are due to the lack of internal radiation once the pour cycle is complete. During the pour phase the internal radiation loss was based on the canister internal surface temperature and the calculated glass temperature.

As seen in the following figures, the temperatures of the glass and the canister surface predicted using the model compare relatively well with the experimental data for both filling and cooling. For the end time of 3000 minutes, the simulations predict a temperature between 30 and 45 ºC (at 15 and 87 inches respectively) higher than the experimental data.

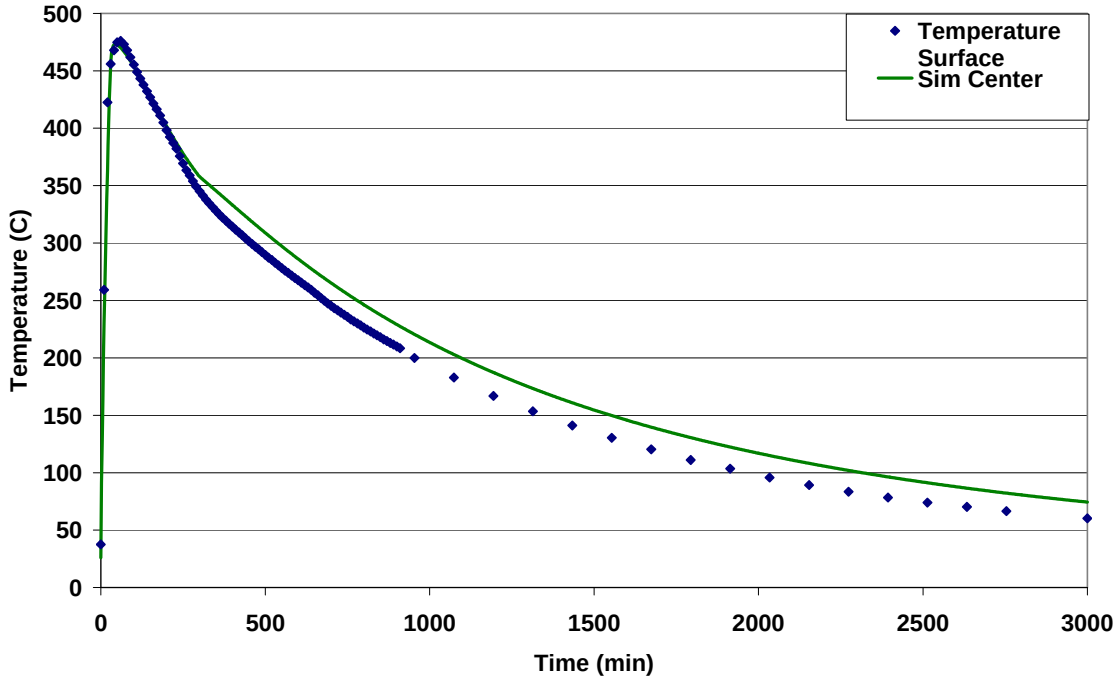

Figure 4 - Temperature curves for thermocouple and simulation data located on the outside bottom of the canister.

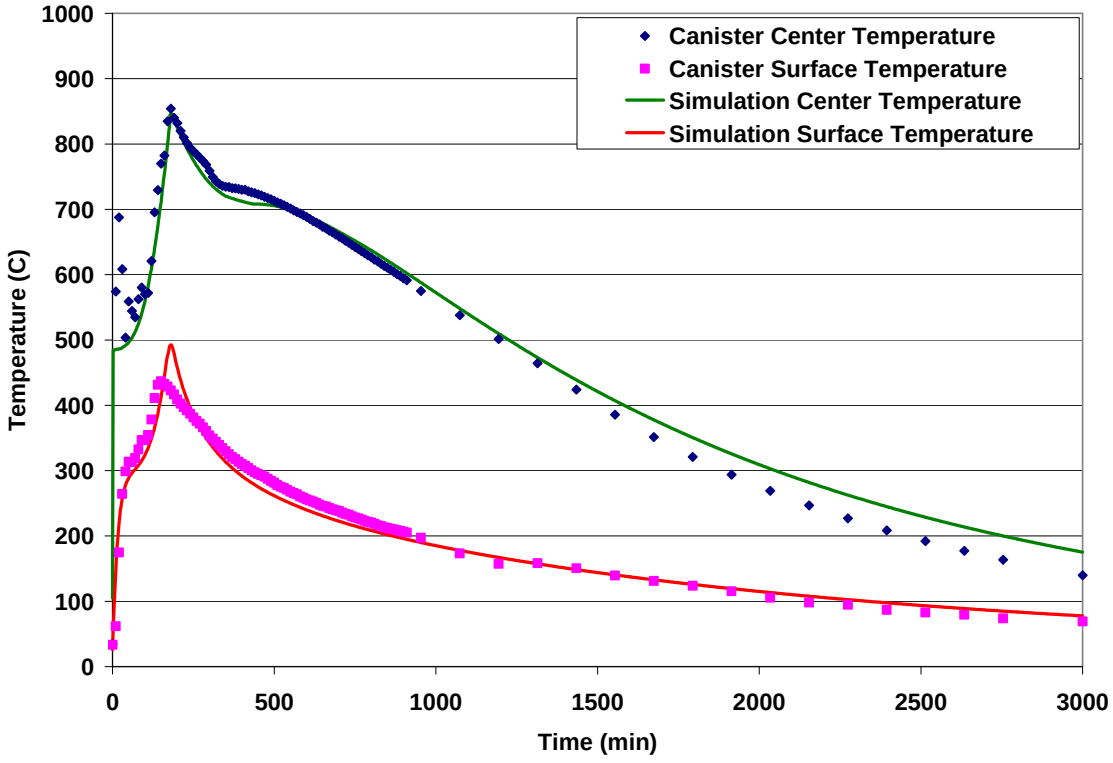

Figure 5 - Temperature curves for thermocouple and simulation data at the 15 inch location of the canister.

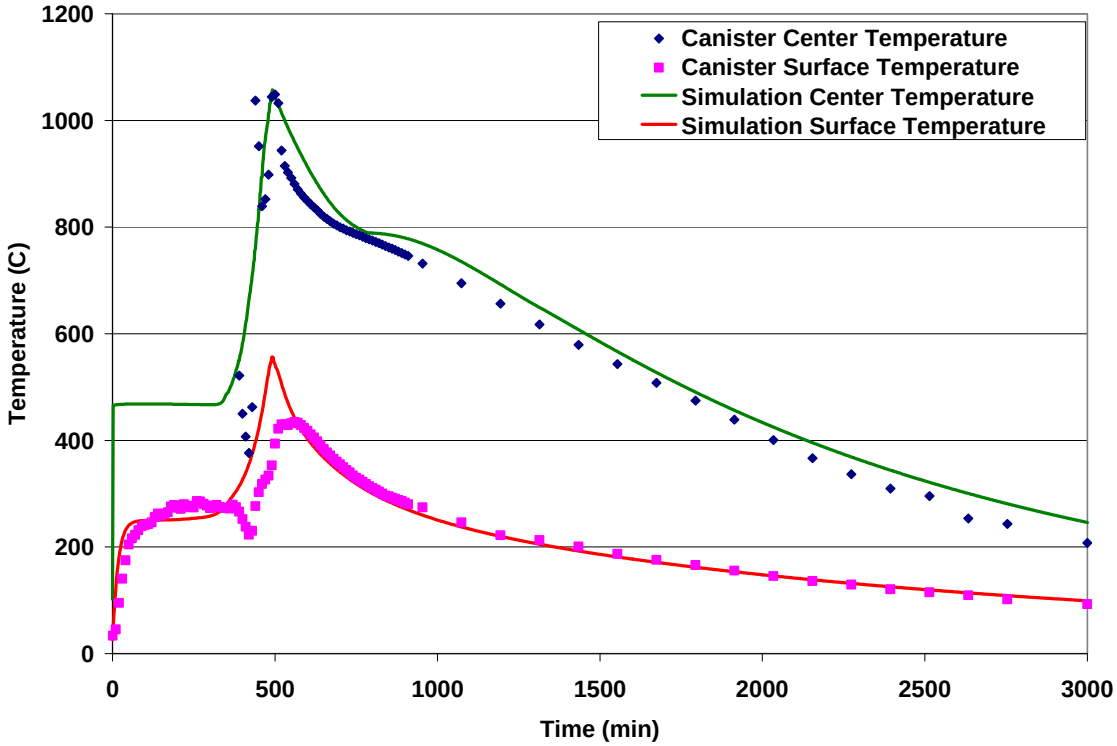

Figure 6 - Temperature curves for thermocouple and simulation data at the 51 inch location of the canister.

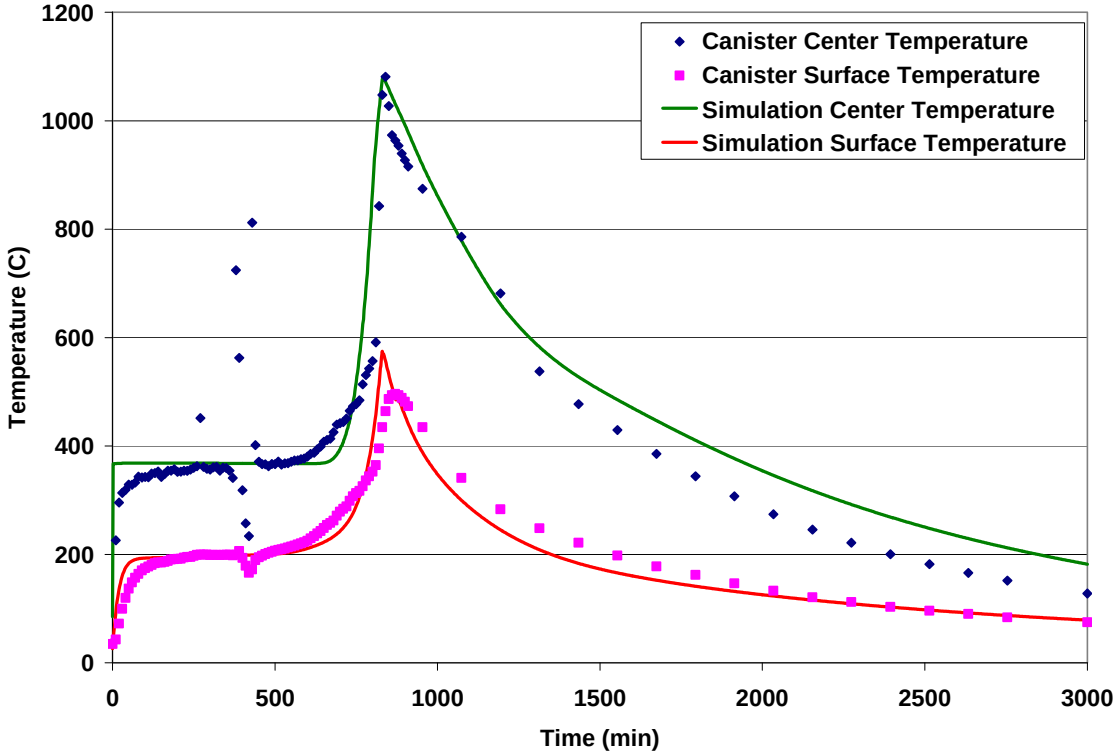

Figure 7 - Temperature curves for thermocouple and simulation data at the 87 inch location of the canister.

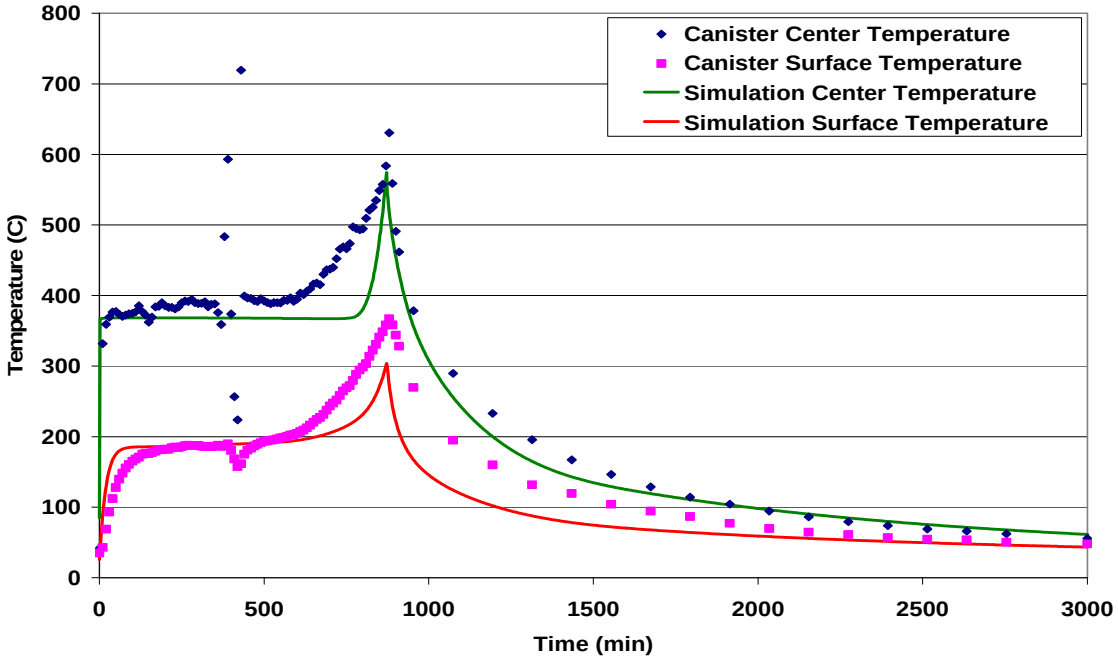

Figure 8 - Temperature curves for thermocouple and simulation data at the 99 inch location of the canister.

6. Conclusions

A COMSOL Multiphysics model was developed to predict temperatures of the glass within DWPF canisters during filling and cooldown. The model simulations and experimental data were in good agreement. The largest temperature deviations were ~ 40°C for the 87inch thermocouple location at 3000 minutes and during the initial cooldown at the 51 inch location occurring at approximately 600 minutes. Additionally, the model described in this report predicts the general trends in temperatures during filling and cooling observed experimentally. However, the model was developed using parameters designed to fit a single set of experimental data. Therefore, Q_loss is not currently a function of pour rate and pour temperature. Future work utilizing the existing model should include modifying the Q_loss term to be variable based on flow rate and pour temperature. Further enhancements could include eliminating the Q_loss term for a user defined convection where Navier-Stokes does not need to be solved in order to have convection heat transfer.

7. References

1. COMSOL Multiphysics, Version 3.5a, COMSOL Inc, Burlington, MA
2. WSRC-IM-91-116-1, “Chemical Composition Projections for then DWPF Product”, 1995, Revision 1, J.R. Fowler, R.E. Edwards, S.L. Marra, M.J. Plodinec
3. Drawing - W747391, “Savannah River Plant Bldg 221S 200 Area DWPF – CDC Canister Assembly Mechanical”, Revision 0, 1984
4. SRNL-L5200-2009-00013, Interoffice Memorandum, “Predicting Temperatures for AFCI Canistered Waste Glasses”, D.A. Tamburello to J.C. Marra

8. Appendix

Appendix A - Comsol Constants and Expressions

The following tables are the constants and global expressions directly exported from COMSOL.

COMSOL Constants

Constant Name	Constant Value
Cp_glass	10[J/g/K]
k_glass	100[W/m/K]
gravity	9.8[m/s^2]
R_ig	.08206[L*atm/mol/K]
MW_air	28.84[g/mol]
glass_k_const	0.6[Btu/h/ft/degF]
glass_rho	167[lb/ft^3]
glass_cp_const	0.2[Btu/lb/degF]
air_k	0.04[Btu/h/ft/degF]
air_cp	0.26[Btu/lb/degF]
glass_visc	10[lb/h/ft]
air_visc	0.1[lb/h/ft]
MW_glass	2000[g/mol]
glass_flow_init_const	228[lb/h]
inlet_area	0.031416[m^2]
Lower_area	0.26512[m^2]
glass_T_init	1080[degC]
sigma	5.67e-8[W/m^2/K^4]
T_atm	26[degC]
Conv_ht	4[W/m^2/K]
SS_rho	494.429[lb/ft^3]
SS_cp_old	.135[Btu/lb/degF]
ContainerHeight	3[m]
Ta	glass_T_init[1/degC]+32
Tb	36.98552
Tc	8.411223
Td	106.379
Q_loss_base	320000[W/m^3]
dt	120[s]
GasHeat	700[W/m^3]
FinalPourSwitch	MaxGlass-500[lb]
MaxGlass	3656[lb]
MaxHeight	MaxGlass/glass_rho/Lower_area
T_Lump_init	200[degC]
int_emmisivity	0.55[1]
Max_Gas_temp	370[degC]
Q_Loss_time	17520[s]
T_amb	25[degC]
T_low	700[degC]
T_high	720[degC]

COMSOL Global Expressions

Vaiable Name	Expression
Cp_eff	air_cp+glass_cp*(z<Fluid_Height)
rho_eff	air_rho+glass_rho_adap*(z<Fluid_Height)
T_ramp	273.15+1[K/s]*t
air_rho	1[atm]/R_ig/T*MW_air
Fluid_Height	(Fluid_Height_new+.01[m])*Filling+MaxHeight*(1-Filling)
HeatFlow	glass_cp*glass_T_init*glass_flow
Fluid_vol	Fluid_Height*Lower_area
Q_rad	emmisivity*view_factor*sigma*((T)^4-(T_atm)^4)+h_surface*(T-T_atm)
delFluidVol	(Fluid_Height-LastFluidHeight)*Lower_area
delHeight	(z<=Fluid_Height)*(z>LastFluidHeight)[1]
Q_glass	(3*(T_glass_top-T)*glass_cp*glass_flow/delFluidVol)*Filling*delHeight*r_factor
Q_calc	(Q_glass-Q_loss*(z<Fluid_Height[m]-.01[m])*(z>Fluid_Height[m]-.8))
glass_k	(0.76449+2.74341*flc2hs(T[1/degC]-950,100))[Btu/h/ft/degF]
glass_rho_adap	(172.31*(T[degC]<20)+(T[degC]>=20)*(T[degC]<=1200)*(172.2011+.00109*T[1/degC]-1.609e-5*(T[1/degC])^2-1.508162e-8*(T[1/degC])^3+1.3323e-11*(T[1/degC])^4)+151.77*(T[degC]>1200))[lb/ft^3]
glass_cp	(0.204+0.16*flc2hs(T[1/degC]-1000,400))[Btu/lb/degF]
glass_T	glass_T_init-25[K/ft]*(3[m]-Fluid_Height)
Q_rad1	emmisivity*view_factor*sigma*((T)^4-(T_atm)^4)
Conv1	h_surface*(T-T_atm)
SS_k	(-13.589083+3.9578316*log(T_min[1/K]))[Btu/h/ft/degF]
Conv_inside	h_surface*(5[K])
Ra_init	gravity*Beta*(T-T_atm)*ContainerHeight^3/(air_visc*air_k/air_rho^2/air_cp)
Ra	Ra_init*(Ra_init>0)
Beta	1/T
Pr	air_cp*air_visc/air_k
h_surface_low	(air_k/ContainerHeight)*(0.68+(0.670*Ra^.25)/(1.0+(0.492/Pr)^(9/16))^(4/9))
h_surface_high	((air_k/ContainerHeight)*(0.825+(0.387*Ra^(1/6))/(1.0+(0.492/Pr)^(9/16))^(8/27))^2)
h_surface	(h_surface_low*(Ra<=1e9)+h_surface_high*(Ra>1e9))
T_min	T*(T>T_atm-5)+T_atm*(T<=T_atm-5)
Internal_rad	int_emmisivity*view_factor2*sigma*((T_interface)^4-(T)^4)*(z>Fluid_Height)*Filling*(T<T_interface)*(0.74-.2*z[1/m])
T_glass_top	(Ta/((1+exp(Tb-Tc*Fluid_Height[1/ft]))^(1/Td)))[degC]*Filling
TopHeat	(glass_T_init-T_atm)*flc2hs((MaxHeight-(LastFluidHeight+.01[m]))[1/m],.2)+T_atm
Filling	((Fluid_Height_new+.01[m])<=MaxHeight)[1]
Q_loss	(Q_loss_base*(-0.0548*(z[1/m])^2+0.1045*z[1/m]+0.48)*(flc2hs(z[1/m]-(Fluid_Height_dummy[1/m]-Q_loss_height[1/m]),(.6568*(z[1/m])^2)-1.5375*z[1/m]+1.7)))*(1/exp(60*(r[1/m])^3))*Q_loss_radial
Q_loss_radial	(r[1/m]>(0.085*z[1/m]+0.0685))*(0.85-.3*z[1/m])*(r<=0.285)+(r[1/m]<=(0.085*z[1/m]+0.0685))
Fluid_Height_dummy	(Fluid_Height_new+.01[m])
T_interface	(glass_T_init-200[K])
TotalGlassPour	glass_flow_init*t
glass_flow	glass_flow_init
glass_flux	glass_flow/MW_glass/inlet_area
glass_flow_rate	glass_flow/glass_rho/Lower_area
view_factor2	0.124-0.03*z[1/m]+.15*(z[1/m])*flc2hs((HF/zF)-.95,.4)

Vaiable Name	Expression
HF	Fluid_Height/MaxHeight
zF	z/MaxHeight
Q_rad_top	sigma*((glass_T_init)^4-(T)^4)*Filling
Gas_Temp	Max_Gas_temp+120*flc2hs(1.5-z[1/m],.5)
Q_gas	(T<Gas_Temp)*2.5*(Gas_Temp-T)*air_cp/(1[s])*air_rho*Filling*(z>(Fluid_Height[m]))*(r<0.2[m])
Q_loss_height	glass_flow_rate*Q_Loss_time/2.5*z[1/m]
view_factor	1[1]
emmisivity	.8[1]
SS_cp	(.12+.015*flc2hs(T[1/degF]-452[degF][1/degF],300))[Btu/lb/degF]
k_eff	(30*air_k)*(z>=Fluid_Height)*Filling*(1-flc2hs((HF/zF)-1.0,.1))+glass_k*flc2hs((HF/zF)-.80,.8)*Filling+(glass_k*(z<=Fluid_Height)+20*air_k*(z>Fluid_Height))*(1-Filling)
T_Hold_Center	((452.2656+240.1336*z[1/m]-40.3449*(z[1/m])^2)*(z<=MaxHeight)+289.5*(z>MaxHeight))[degC]
T_Hold_Surface	((148.5466+60.03426*z[1/m]+12.26439*(z[1/m])^2)*(z<=MaxHeight)+194.8*(z>MaxHeight))[degC]
T_3inch	(445.1069+187.7072*z[1/m]-13.2499*(z[1/m])^2)[degC]
T_6inch	(388.567+125.6953*z[1/m]+20.96399*(z[1/m])^2)[degC]
T_9inch	(282.3685+103.7025*z[1/m]+25.63263*(z[1/m])^2)[degC]
SteadyQ	T_3inch*(r<.0764)*(r>.076)+T_6inch*(r<.1526)*(r>.1522)+T_9inch*(r<.2288)*(r>.2284)
glass_flow_init	(201+120*(t>=180*60)+40*(t>=270*60)-170*(t>=350*60)+70*(t>=500*60)-20*(t>=610*60)+20*(t>=730+60))[lb/h]
glassFlow1	201[lb/h]*t*(t<=180[min])
glassFlow2	(321.5[lb/h]*(t-180[min])+glw1)*(t>180[min])*(t<=270[min])
glassFlow3	(361.7[lb/h]*(t-270[min])+glw1+glw2)*(t>270[min])*(t<=350[min])
glassFlow4	(192.9[lb/h]*(t-350[min])+glw1+glw2+glw3)*(t>350[min])*(t<=500[min])
glassFlow5	(263.1[lb/h]*(t-500[min])+glw1+glw2+glw3+glw4)*(t>500[min])*(t<=610[min])
glassFlow6	(241.1[lb/h]*(t-610[min])+glw1+glw2+glw3+glw4+glw5)*(t>610[min])*(t<=730[min])
glassFlow7	(263.1[lb/h]*(t-730[min])+glw1+glw2+glw3+glw4+glw5+glw6)*(t>730[min])
glw1	201[lb/h]*180[min]
glw2	321.5[lb/h]*90[min]
glw3	361.7[lb/h]*80[min]
glw4	192.9[lb/h]*150[min]
glw5	263.1[lb/h]*110[min]
glw6	241.1[lb/h]*120[min]
Fluid_Height_new	(glassFlow1+glassFlow2+glassFlow3+glassFlow4+glassFlow5+glassFlow6+glassFlow7)/glass_rho/Lower_area
glassFlow1_dt	201[lb/h]*(t-dt)*(t<=180[min])
glassFlow2_dt	(321.5[lb/h]*(t-dt-180[min])+glw1)*(t>180[min])*(t<=270[min])
glassFlow3_dt	(361.7[lb/h]*(t-dt-270[min])+glw1+glw2)*(t>270[min])*(t<=350[min])
glassFlow4_dt	(192.9[lb/h]*(t-dt-350[min])+glw1+glw2+glw3)*(t>350[min])*(t<=500[min])
glassFlow5_dt	(263.1[lb/h]*(t-dt-500[min])+glw1+glw2+glw3+glw4)*(t>500[min])*(t<=610[min])
glassFlow6_dt	(241.1[lb/h]*(t-dt-610[min])+glw1+glw2+glw3+glw4+glw5)*(t>610[min])*(t<=730[min])
glassFlow7_dt	(263.1[lb/h]*(t-dt-730[min])+glw1+glw2+glw3+glw4+glw5+glw6)*(t>730[min])
LastFluidHeight	((glassFlow1_dt+glassFlow2_dt+glassFlow3_dt+glassFlow4_dt+glassFlow5_dt+glassFlow6_dt+glassFlow7_dt)/glass_rho/Lower_area)
r_factor	1-r[1/m]/2*z[1/m][1]
R1_old	flc2hs(T[1/degC]-T_low[1/degC],1)*flc2hs(T_high[1/degC]-T[1/degC],1)*0.001[mol/s/m^3]
R1	(T>T_low)*(T<T_high)*0.0001[mol/s/m^3]

Appendix B - Simulation Temperature versus Time Data

Time (min)	Bottom (C)	15 Inch Center (C)	15 inch Surface (C)	51 inch Center (C)	51 inch Surface (C)	87 inch Center (C)	87 inch Surface (C)	99 inch Center (C)	99 inch Surface (C)
0	25.9	26.0	26.0	26.0	26.0	26.0	26.0	26.0	26.0
10	230.1	132.5	86.9	58.3	58.5	39.9	39.7	37.4	35.3
20	362.9	487.8	160.3	469.4	111.7	369.2	72.4	369.2	64.4
30	457.5	491.5	224.8	471.5	167.6	370.0	111.6	370.0	101.6
40	472.8	496.8	262.3	471.5	203.1	370.0	139.5	370.0	128.4
50	472.7	504.2	283.3	471.5	223.9	370.0	157.9	370.0	146.6
60	470.3	514.0	295.9	471.5	235.6	370.0	169.7	370.0	158.6
70	466.9	524.5	304.9	471.5	242.1	370.0	177.0	370.0	166.4
80	462.9	538.4	313.0	471.5	245.8	370.0	181.6	370.0	171.4
90	458.5	555.2	321.8	471.5	247.8	370.0	184.5	370.0	174.5
100	453.8	573.9	332.2	471.5	249.0	370.0	186.2	370.0	176.5
110	448.9	595.2	344.6	471.5	249.7	370.0	187.3	370.0	177.7
120	443.9	619.2	360.0	471.5	250.2	370.0	188.0	370.0	178.4
130	438.7	647.8	378.0	471.5	250.5	370.0	188.4	370.0	178.9
140	433.4	678.9	398.6	471.5	250.8	370.0	188.7	370.0	179.2
150	428.1	730.3	421.7	471.5	251.1	370.0	188.9	370.0	179.5
160	422.8	792.7	445.1	471.5	251.4	370.0	189.1	370.0	179.6
170	417.5	833.5	460.1	471.5	251.7	370.0	189.2	370.0	179.7
180	412.2	848.2	459.9	471.5	252.1	370.0	189.3	370.0	179.8
190	406.9	837.3	453.8	471.4	252.5	370.0	189.5	370.0	179.9
200	401.8	826.0	440.0	471.4	253.0	370.0	189.6	370.0	180.0
210	396.8	815.3	425.8	471.4	253.6	370.0	189.8	370.0	180.2
220	391.9	805.2	412.6	471.4	254.2	370.0	190.0	370.0	180.3
230	387.1	795.7	400.5	471.4	255.0	370.0	190.2	370.0	180.5
240	382.5	786.7	389.7	471.4	255.7	370.0	190.4	370.0	180.7
250	378.0	778.3	379.8	471.4	256.6	370.0	190.7	370.0	180.9
260	373.7	770.6	370.9	471.3	257.4	370.0	191.0	370.0	181.1
270	369.5	763.4	362.7	471.3	258.5	370.0	191.3	370.0	181.3
280	365.5	756.5	355.2	471.3	259.7	370.0	191.6	370.0	181.6
290	361.6	750.3	348.2	471.3	261.4	370.0	192.0	370.0	181.9
300	358.0	744.7	341.8	471.3	263.6	369.9	192.4	370.0	182.2
310	355.4	739.6	335.7	471.4	266.6	369.9	192.8	369.9	182.6
320	353.0	735.1	330.1	471.9	270.4	369.9	193.3	369.9	183.0
330	350.5	731.0	324.8	474.7	275.1	369.9	193.8	369.9	183.4
340	348.1	727.5	319.8	481.6	281.1	369.9	194.3	369.9	183.8
350	345.6	724.4	315.2	494.5	288.7	369.9	194.8	369.9	184.2
360	343.1	722.4	310.8	504.8	297.2	369.9	195.3	369.9	184.6
370	340.6	720.6	306.7	519.2	305.3	369.9	195.8	369.9	185.0
380	338.2	718.9	302.8	536.9	313.5	369.9	196.1	369.9	185.3
390	335.7	717.3	299.1	557.7	322.7	369.9	196.5	369.9	185.6
400	333.2	715.9	295.6	583.0	333.5	369.9	196.9	369.9	185.9

Time (min)	Bottom (C)	15 Inch Center (C)	15 inch Surface (C)	51 inch Center (C)	51 inch Surface (C)	87 inch Center (C)	87 inch Surface (C)	99 inch Center (C)	99 inch Surface (C)
410	330.7	715.6	292.2	616.7	346.0	369.9	197.2	369.9	186.2
420	328.3	715.7	289.1	654.8	360.8	369.9	197.5	369.9	186.5
430	325.8	715.7	286.1	699.2	378.5	369.9	197.9	369.9	186.8
440	323.4	715.5	283.2	765.4	399.3	369.9	198.3	369.9	187.1
450	320.9	715.2	280.4	857.4	424.5	369.9	198.6	369.9	187.4
460	318.5	714.8	277.7	953.9	452.7	369.9	199.1	369.9	187.7
470	316.1	714.2	275.1	1017.0	481.2	369.9	199.5	369.9	188.0
480	313.7	713.4	272.5	1050.6	501.6	369.9	200.0	369.9	188.3
490	311.3	712.5	270.1	1056.6	506.0	369.9	200.5	369.9	188.6
500	308.9	711.5	267.7	1040.5	496.3	369.9	201.1	369.9	188.9
510	306.6	710.3	265.4	1024.7	486.0	369.9	201.9	369.9	189.3
520	304.2	709.0	263.2	1009.4	473.3	369.9	202.8	369.9	189.7
530	301.9	707.5	261.0	994.8	460.7	369.9	203.9	369.9	190.1
540	299.6	705.9	258.9	980.7	449.0	369.9	205.1	369.9	190.6
550	297.3	704.2	256.8	967.1	438.2	369.9	206.6	369.9	191.2
560	295.1	702.4	254.8	954.0	428.3	369.9	208.2	369.9	191.8
570	292.8	700.5	252.8	941.3	419.2	369.9	210.0	369.9	192.6
580	290.6	698.5	250.9	928.8	410.8	369.9	212.0	369.9	193.4
590	288.4	696.4	249.0	916.5	403.0	369.9	214.1	369.9	194.3
600	286.2	694.1	247.2	904.5	395.7	370.0	216.5	369.9	195.3
610	284.0	691.8	245.3	892.6	388.8	370.2	219.0	369.9	196.4
620	281.8	689.5	243.6	881.6	382.3	370.8	221.7	369.9	197.6
630	279.7	687.0	241.9	870.9	376.2	371.8	224.4	369.9	198.9
640	277.6	684.5	240.2	860.5	370.3	373.5	227.4	369.9	200.2
650	275.5	681.9	238.5	850.6	364.7	376.2	230.6	369.9	201.7
660	273.4	679.2	236.9	841.4	359.4	380.2	234.1	369.9	203.2
670	271.3	676.5	235.3	832.8	354.2	386.1	237.9	369.9	204.9
680	269.3	673.7	233.7	824.8	349.3	394.4	242.3	369.9	206.7
690	267.3	670.9	232.2	817.3	344.5	405.3	247.2	369.9	208.5
700	265.3	668.0	230.6	810.5	340.0	419.9	252.8	369.9	210.5
710	263.3	665.2	229.2	804.3	335.6	439.1	259.4	369.9	212.5
720	261.3	662.3	227.7	798.6	331.3	462.7	267.1	370.0	214.7
730	259.4	659.3	226.2	793.4	327.2	491.9	276.1	370.2	217.0
740	257.5	656.4	224.8	788.7	323.3	525.4	286.4	370.6	219.4
750	255.6	653.5	223.4	784.5	319.5	567.8	298.3	371.5	222.1
760	253.7	650.6	222.1	780.9	315.9	621.8	312.1	373.2	224.9
770	251.8	647.6	220.7	779.7	312.4	687.0	328.7	375.9	228.0
780	249.9	644.6	219.4	779.6	309.1	766.3	348.6	380.0	231.4
790	248.1	641.5	218.1	779.4	305.9	861.5	373.1	386.0	235.2
800	246.3	638.4	216.8	779.1	302.9	955.1	404.4	394.7	239.4
810	244.5	635.2	215.5	778.7	299.9	1024.7	443.2	407.4	244.3
820	242.7	632.1	214.2	778.2	297.0	1074.7	481.2	424.2	250.1
830	240.9	628.9	213.0	777.6	294.2	1093.7	498.3	446.0	257.0
840	239.2	625.7	211.8	776.9	291.5	1076.2	489.4	473.2	265.1
850	237.5	622.4	210.6	776.1	288.9	1058.4	475.1	508.0	274.8
860	235.8	619.1	209.4	775.1	286.4	1040.8	461.0	553.3	286.4
870	234.1	615.9	208.2	774.0	283.9	1023.6	448.1	606.5	300.3

Time (min)	Bottom (C)	15 Inch Center (C)	15 inch Surface (C)	51 inch Center (C)	51 inch Surface (C)	87 inch Center (C)	87 inch Surface (C)	99 inch Center (C)	99 inch Surface (C)
880	232.4	612.6	207.0	772.8	281.5	1006.7	447.3	593.7	329.4
890	230.7	609.3	205.9	771.5	279.1	990.4	439.1	580.5	340.0
900	229.1	605.9	204.8	770.0	276.8	974.2	428.7	564.9	338.6
910	227.4	602.6	203.6	768.4	274.6	957.9	418.2	548.4	333.0
920	225.8	599.2	202.5	766.7	272.5	941.7	408.1	531.7	325.9
930	224.2	595.9	201.4	764.9	270.3	925.8	398.6	515.2	318.3
940	222.7	592.5	200.4	763.0	268.3	910.3	389.5	499.7	310.5
950	221.1	589.2	199.3	760.9	266.3	895.1	381.0	485.3	302.8
960	219.5	585.8	198.2	758.8	264.3	880.2	372.8	471.8	295.1
970	218.0	582.4	197.2	756.5	262.4	865.5	365.1	459.0	287.6
980	216.5	579.1	196.1	754.1	260.5	851.1	357.7	446.7	280.2
990	215.0	575.7	195.1	751.7	258.7	836.8	350.6	434.8	272.9
1000	213.5	572.3	194.1	749.1	256.9	822.8	343.8	423.3	265.8
1010	212.0	569.0	193.1	746.5	255.1	808.9	337.3	412.2	258.7
1020	210.5	565.6	192.1	743.8	253.4	795.3	331.0	401.4	251.8
1030	209.1	562.3	191.1	741.0	251.7	781.9	325.0	390.9	245.0
1040	207.7	558.9	190.1	738.1	250.1	768.7	319.1	380.8	238.3
1050	206.2	555.6	189.2	735.1	248.5	755.8	313.5	370.9	231.8
1060	204.8	552.2	188.2	732.1	246.9	743.1	308.0	361.5	225.3
1070	203.4	548.9	187.3	729.1	245.3	730.6	302.7	352.3	219.0
1080	202.1	545.6	186.3	725.9	243.8	718.3	297.5	343.4	212.8
1090	200.7	542.3	185.4	722.8	242.3	706.3	292.5	334.7	206.7
1100	199.4	539.0	184.5	719.5	240.8	694.6	287.7	326.4	200.8
1110	198.0	535.7	183.6	716.2	239.4	683.2	283.0	318.2	195.0
1120	196.7	532.4	182.7	712.9	237.9	672.0	278.4	310.3	189.3
1130	195.4	529.1	181.8	709.6	236.5	661.1	274.0	302.6	183.7
1140	194.1	525.8	180.9	706.2	235.2	651.0	269.6	295.2	178.3
1150	192.8	522.6	180.0	702.7	233.8	641.6	265.4	288.0	173.1
1160	191.5	519.4	179.1	699.3	232.5	632.5	261.4	280.9	167.9
1170	190.3	516.1	178.3	695.8	231.1	623.8	257.4	274.2	162.9
1180	189.0	512.9	177.4	692.3	229.9	615.3	253.5	267.6	158.0
1190	187.8	509.7	176.5	688.8	228.6	607.1	249.8	261.2	153.3
1200	186.5	506.6	175.7	685.3	227.3	599.2	246.1	255.1	148.8
1210	185.3	503.4	174.9	681.8	226.1	591.6	242.6	249.2	144.3
1220	184.1	500.3	174.0	678.2	224.9	584.3	239.2	243.4	140.0
1230	182.9	497.1	173.2	674.7	223.6	577.2	235.8	237.9	135.9
1240	181.7	494.0	172.4	671.2	222.5	570.4	232.6	232.6	131.9
1250	180.6	490.9	171.6	667.7	221.3	563.8	229.4	227.5	128.1
1260	179.4	487.8	170.8	664.2	220.1	557.5	226.4	222.6	124.4
1270	178.3	484.7	169.9	660.7	219.0	551.5	223.4	217.8	120.8
1280	177.1	481.7	169.2	657.3	217.8	545.6	220.6	213.3	117.4
1290	176.0	478.6	168.4	654.0	216.7	540.1	217.8	208.9	114.1
1300	174.9	475.6	167.6	650.8	215.6	534.7	215.1	204.7	111.0
1310	173.8	472.6	166.8	647.6	214.5	529.6	212.5	200.7	108.0
1320	172.7	469.6	166.0	644.2	213.5	524.6	209.9	196.9	105.2
1330	171.6	466.7	165.3	640.9	212.4	519.9	207.5	193.2	102.5
1340	170.5	463.7	164.5	637.5	211.3	515.4	205.1	189.7	99.9

Time (min)	Bottom (C)	15 Inch Center (C)	15 inch Surface (C)	51 inch Center (C)	51 inch Surface (C)	87 inch Center (C)	87 inch Surface (C)	99 inch Center (C)	99 inch Surface (C)
1350	169.4	460.8	163.7	634.2	210.3	511.0	202.8	186.4	97.4
1360	168.4	457.9	163.0	630.8	209.3	506.9	200.6	183.2	95.1
1370	167.3	455.0	162.2	627.4	208.2	502.8	198.4	180.2	92.9
1380	166.3	452.1	161.5	624.0	207.2	499.0	196.3	177.3	90.8
1390	165.3	449.2	160.8	620.6	206.2	495.3	194.3	174.6	88.9
1400	164.3	446.4	160.0	617.2	205.3	491.8	192.4	172.0	87.0
1410	163.3	443.5	159.3	613.8	204.3	488.3	190.5	169.5	85.3
1420	162.3	440.7	158.6	610.4	203.3	485.0	188.7	167.2	83.6
1430	161.3	437.9	157.9	607.0	202.3	481.8	186.9	165.0	82.1
1440	160.3	435.1	157.1	603.6	201.4	478.8	185.2	162.9	80.7
1450	159.3	432.4	156.4	600.2	200.5	475.8	183.5	160.9	79.3
1460	158.3	429.6	155.7	596.8	199.5	472.9	181.9	159.0	78.1
1470	157.4	426.9	155.0	593.4	198.6	470.0	180.4	157.2	76.9
1480	156.4	424.2	154.3	590.1	197.7	467.3	178.9	155.5	75.8
1490	155.5	421.5	153.7	586.7	196.8	464.6	177.4	153.9	74.8
1500	154.6	418.9	153.0	583.3	195.9	461.9	176.0	152.4	73.9
1510	153.6	416.2	152.3	580.0	195.0	459.3	174.6	151.0	73.0
1520	152.7	413.6	151.6	576.7	194.1	456.7	173.3	149.6	72.2
1530	151.8	411.0	150.9	573.3	193.2	454.2	172.0	148.4	71.5
1540	150.9	408.4	150.3	570.0	192.4	451.7	170.7	147.2	70.9
1550	150.0	405.8	149.6	566.7	191.5	449.2	169.5	146.1	70.3
1560	149.2	403.2	148.9	563.4	190.7	446.7	168.3	145.0	69.8
1570	148.3	400.7	148.3	560.2	189.8	444.2	167.1	144.0	69.3
1580	147.4	398.1	147.6	556.9	189.0	441.8	166.0	143.0	68.8
1590	146.6	395.6	147.0	553.7	188.1	439.3	164.9	142.1	68.4
1600	145.7	393.1	146.3	550.4	187.3	436.9	163.8	141.1	68.0
1610	144.9	390.7	145.7	547.2	186.5	434.4	162.7	140.3	67.6
1620	144.0	388.2	145.1	544.0	185.7	431.9	161.7	139.4	67.3
1630	143.2	385.7	144.4	540.8	184.9	429.5	160.7	138.6	66.9
1640	142.4	383.3	143.8	537.6	184.1	427.0	159.7	137.8	66.6
1650	141.6	380.9	143.2	534.5	183.3	424.6	158.7	136.9	66.2
1660	140.7	378.5	142.6	531.3	182.5	422.1	157.7	136.2	65.9
1670	139.9	376.1	141.9	528.2	181.7	419.7	156.8	135.4	65.6
1680	139.1	373.8	141.3	525.1	180.9	417.3	155.9	134.6	65.3
1690	138.4	371.5	140.7	522.0	180.2	414.8	155.0	133.9	65.0
1700	137.6	369.1	140.1	518.9	179.4	412.4	154.1	133.1	64.7
1710	136.8	366.8	139.5	515.9	178.6	410.0	153.2	132.4	64.5
1720	136.0	364.5	138.9	512.8	177.9	407.6	152.3	131.6	64.2
1730	135.3	362.3	138.3	509.8	177.1	405.2	151.4	130.9	63.9
1740	134.5	360.0	137.7	506.8	176.4	402.8	150.6	130.2	63.7
1750	133.8	357.8	137.1	503.8	175.6	400.4	149.8	129.4	63.4
1760	133.0	355.5	136.5	500.8	174.9	398.0	148.9	128.7	63.2
1770	132.3	353.3	136.0	497.8	174.2	395.6	148.1	128.0	62.9
1780	131.6	351.1	135.4	494.9	173.4	393.2	147.3	127.3	62.7
1790	130.8	348.9	134.8	492.0	172.7	390.8	146.5	126.6	62.4
1800	130.1	346.8	134.2	489.1	172.0	388.5	145.8	125.9	62.2
1810	129.4	344.6	133.7	486.2	171.3	386.1	145.0	125.2	61.9

Time (min)	Bottom (C)	15 Inch Center (C)	15 inch Surface (C)	51 inch Center (C)	51 inch Surface (C)	87 inch Center (C)	87 inch Surface (C)	99 inch Center (C)	99 inch Surface (C)
1820	128.7	342.5	133.1	483.3	170.6	383.8	144.2	124.5	61.7
1830	128.0	340.4	132.5	480.5	169.9	381.4	143.5	123.8	61.5
1840	127.3	338.3	132.0	477.6	169.2	379.1	142.7	123.1	61.2
1850	126.6	336.2	131.4	474.8	168.5	376.8	142.0	122.5	61.0
1860	125.9	334.1	130.9	472.0	167.8	374.5	141.3	121.8	60.8
1870	125.3	332.1	130.3	469.2	167.1	372.2	140.5	121.1	60.6
1880	124.6	330.0	129.8	466.4	166.4	369.9	139.8	120.5	60.3
1890	123.9	328.0	129.2	463.7	165.7	367.6	139.1	119.8	60.1
1900	123.3	326.0	128.7	461.0	165.1	365.4	138.4	119.2	59.9
1910	122.6	324.0	128.1	458.2	164.4	363.1	137.7	118.5	59.7
1920	121.9	322.0	127.6	455.5	163.7	360.9	137.0	117.9	59.5
1930	121.3	320.1	127.1	452.9	163.1	358.6	136.4	117.3	59.3
1940	120.7	318.1	126.5	450.2	162.4	356.4	135.7	116.6	59.1
1950	120.0	316.2	126.0	447.5	161.7	354.2	135.0	116.0	58.8
1960	119.4	314.3	125.5	444.9	161.1	352.0	134.4	115.4	58.6
1970	118.8	312.3	125.0	442.3	160.4	349.8	133.7	114.8	58.4
1980	118.2	310.5	124.4	439.7	159.8	347.7	133.1	114.2	58.2
1990	117.5	308.6	123.9	437.1	159.2	345.5	132.4	113.6	58.0
2000	116.9	306.7	123.4	434.6	158.5	343.3	131.8	113.0	57.8
2010	116.3	304.9	122.9	432.0	157.9	341.2	131.2	112.4	57.6
2020	115.7	303.0	122.4	429.5	157.3	339.1	130.6	111.8	57.5
2030	115.1	301.2	121.9	427.0	156.6	337.0	129.9	111.2	57.3
2040	114.5	299.4	121.4	424.5	156.0	334.9	129.3	110.6	57.1
2050	114.0	297.6	120.9	422.0	155.4	332.8	128.7	110.1	56.9
2060	113.4	295.8	120.4	419.5	154.8	330.7	128.1	109.5	56.7
2070	112.8	294.0	119.9	417.1	154.2	328.7	127.5	108.9	56.5
2080	112.2	292.3	119.4	414.7	153.6	326.6	126.9	108.4	56.3
2090	111.7	290.5	118.9	412.3	153.0	324.6	126.3	107.8	56.1
2100	111.1	288.8	118.5	409.9	152.3	322.6	125.8	107.3	56.0
2110	110.5	287.0	118.0	407.5	151.7	320.6	125.2	106.7	55.8
2120	110.0	285.3	117.5	405.1	151.2	318.6	124.6	106.2	55.6
2130	109.4	283.6	117.0	402.8	150.6	316.6	124.0	105.6	55.4
2140	108.9	282.0	116.5	400.4	150.0	314.7	123.5	105.1	55.2
2150	108.3	280.3	116.1	398.1	149.4	312.7	122.9	104.5	55.1
2160	107.8	278.6	115.6	395.8	148.8	310.8	122.4	104.0	54.9
2170	107.3	277.0	115.1	393.5	148.2	308.8	121.8	103.5	54.7
2180	106.7	275.3	114.7	391.3	147.6	306.9	121.3	103.0	54.6
2190	106.2	273.7	114.2	389.0	147.1	305.0	120.7	102.5	54.4
2200	105.7	272.1	113.8	386.8	146.5	303.2	120.2	102.0	54.2
2210	105.2	270.5	113.3	384.6	145.9	301.3	119.7	101.4	54.1
2220	104.7	268.9	112.9	382.3	145.4	299.4	119.1	100.9	53.9
2230	104.2	267.4	112.4	380.2	144.8	297.6	118.6	100.4	53.7
2240	103.7	265.8	112.0	378.0	144.2	295.7	118.1	99.9	53.6
2250	103.1	264.2	111.5	375.8	143.7	293.9	117.6	99.5	53.4
2260	102.7	262.7	111.1	373.7	143.1	292.1	117.1	99.0	53.2
2270	102.2	261.2	110.6	371.5	142.6	290.3	116.5	98.5	53.1
2280	101.7	259.6	110.2	369.4	142.0	288.5	116.0	98.0	52.9

Time (min)	Bottom (C)	15 Inch Center (C)	15 inch Surface (C)	51 inch Center (C)	51 inch Surface (C)	87 inch Center (C)	87 inch Surface (C)	99 inch Center (C)	99 inch Surface (C)
2290	101.2	258.1	109.8	367.3	141.5	286.8	115.5	97.5	52.8
2300	100.7	256.6	109.3	365.2	140.9	285.0	115.0	97.1	52.6
2310	100.2	255.2	108.9	363.1	140.4	283.3	114.5	96.6	52.5
2320	99.7	253.7	108.5	361.1	139.9	281.6	114.0	96.1	52.3
2330	99.3	252.2	108.0	359.0	139.3	279.8	113.6	95.7	52.2
2340	98.8	250.8	107.6	357.0	138.8	278.1	113.1	95.2	52.0
2350	98.3	249.3	107.2	355.0	138.3	276.4	112.6	94.8	51.9
2360	97.9	247.9	106.8	353.0	137.7	274.8	112.1	94.3	51.7
2370	97.4	246.5	106.3	351.0	137.2	273.1	111.6	93.9	51.6
2380	97.0	245.0	105.9	349.0	136.7	271.4	111.2	93.4	51.4
2390	96.5	243.6	105.5	347.1	136.2	269.8	110.7	93.0	51.3
2400	96.1	242.3	105.1	345.1	135.7	268.2	110.2	92.5	51.1
2410	95.6	240.9	104.7	343.2	135.1	266.6	109.8	92.1	51.0
2420	95.2	239.5	104.3	341.2	134.6	265.0	109.3	91.7	50.8
2430	94.7	238.1	103.9	339.3	134.1	263.4	108.8	91.2	50.7
2440	94.3	236.8	103.5	337.4	133.6	261.8	108.4	90.8	50.5
2450	93.9	235.4	103.1	335.5	133.1	260.2	107.9	90.4	50.4
2460	93.5	234.1	102.7	333.7	132.6	258.7	107.5	90.0	50.3
2470	93.0	232.8	102.3	331.8	132.1	257.1	107.0	89.6	50.1
2480	92.6	231.5	101.9	330.0	131.6	255.6	106.6	89.2	50.0
2490	92.2	230.2	101.5	328.1	131.1	254.0	106.1	88.8	49.9
2500	91.8	228.9	101.1	326.3	130.6	252.5	105.7	88.3	49.7
2510	91.4	227.6	100.7	324.5	130.1	251.0	105.3	87.9	49.6
2520	91.0	226.3	100.4	322.7	129.7	249.5	104.8	87.6	49.5
2530	90.5	225.1	100.0	320.9	129.2	248.1	104.4	87.2	49.3
2540	90.1	223.8	99.6	319.2	128.7	246.6	104.0	86.8	49.2
2550	89.7	222.6	99.2	317.4	128.2	245.1	103.6	86.4	49.1
2560	89.3	221.3	98.8	315.7	127.7	243.7	103.1	86.0	48.9
2570	88.9	220.1	98.5	313.9	127.3	242.3	102.7	85.6	48.8
2580	88.6	218.9	98.1	312.2	126.8	240.8	102.3	85.2	48.7
2590	88.2	217.7	97.7	310.5	126.3	239.4	101.9	84.8	48.6
2600	87.8	216.4	97.4	308.8	125.9	238.0	101.5	84.5	48.4
2610	87.4	215.3	97.0	307.1	125.4	236.6	101.1	84.1	48.3
2620	87.0	214.1	96.6	305.4	124.9	235.3	100.7	83.7	48.2
2630	86.6	212.9	96.3	303.8	124.5	233.9	100.3	83.4	48.1
2640	86.3	211.7	95.9	302.1	124.0	232.5	99.9	83.0	47.9
2650	85.9	210.6	95.5	300.5	123.5	231.2	99.5	82.6	47.8
2660	85.5	209.4	95.2	298.8	123.1	229.8	99.1	82.3	47.7
2670	85.2	208.3	94.8	297.2	122.6	228.5	98.7	81.9	47.6
2680	84.8	207.1	94.5	295.6	122.2	227.2	98.3	81.6	47.5
2690	84.4	206.0	94.1	294.0	121.7	225.9	97.9	81.2	47.3
2700	84.1	204.9	93.8	292.4	121.3	224.6	97.5	80.9	47.2
2710	83.7	203.8	93.4	290.8	120.9	223.3	97.1	80.5	47.1
2720	83.4	202.7	93.1	289.3	120.4	222.0	96.8	80.2	47.0
2730	83.0	201.6	92.8	287.7	120.0	220.7	96.4	79.9	46.9
2740	82.7	200.5	92.4	286.2	119.5	219.5	96.0	79.5	46.8
2750	82.3	199.4	92.1	284.6	119.1	218.2	95.6	79.2	46.6

Time (min)	Bottom (C)	15 Inch Center (C)	15 inch Surface (C)	51 inch Center (C)	51 inch Surface (C)	87 inch Center (C)	87 inch Surface (C)	99 inch Center (C)	99 inch Surface (C)
2760	82.0	198.3	91.7	283.1	118.7	217.0	95.3	78.8	46.5
2770	81.6	197.2	91.4	281.6	118.2	215.7	94.9	78.5	46.4
2780	81.3	196.2	91.1	280.1	117.8	214.5	94.5	78.2	46.3
2790	81.0	195.1	90.7	278.6	117.4	213.3	94.2	77.9	46.2
2800	80.6	194.1	90.4	277.1	117.0	212.1	93.8	77.5	46.1
2810	80.3	193.1	90.1	275.6	116.5	210.9	93.4	77.2	46.0
2820	80.0	192.0	89.7	274.2	116.1	209.7	93.1	76.9	45.9
2830	79.6	191.0	89.4	272.7	115.7	208.5	92.7	76.6	45.8
2840	79.3	190.0	89.1	271.3	115.3	207.4	92.4	76.3	45.7
2850	79.0	189.0	88.8	269.9	114.9	206.2	92.0	76.0	45.5
2860	78.7	188.0	88.5	268.4	114.5	205.0	91.7	75.7	45.4
2870	78.3	187.0	88.1	267.0	114.1	203.9	91.3	75.4	45.3
2880	78.0	186.0	87.8	265.6	113.6	202.8	91.0	75.0	45.2
2890	77.7	185.0	87.5	264.2	113.2	201.6	90.6	74.7	45.1
2900	77.4	184.1	87.2	262.8	112.8	200.5	90.3	74.4	45.0
2910	77.1	183.1	86.9	261.4	112.4	199.4	89.9	74.2	44.9
2920	76.8	182.1	86.6	260.1	112.0	198.3	89.6	73.9	44.8
2930	76.5	181.2	86.3	258.7	111.6	197.2	89.3	73.6	44.7
2940	76.2	180.2	86.0	257.4	111.2	196.1	88.9	73.3	44.6
2950	75.9	179.3	85.7	256.0	110.8	195.0	88.6	73.0	44.5
2960	75.6	178.4	85.4	254.7	110.5	194.0	88.3	72.7	44.4
2970	75.3	177.4	85.1	253.4	110.1	192.9	87.9	72.4	44.3
2980	75.0	176.5	84.8	252.1	109.7	191.8	87.6	72.1	44.2
2990	74.7	175.6	84.5	250.8	109.3	190.8	87.3	71.8	44.1
3000	74.4	174.7	84.2	249.5	108.9	189.8	87.0	71.6	44.0

Distribution

J. W. Amoroso, 999-W
A. B. Barnes, 999-W
A. L. Billings, 999-W
C. L. Crawford, 773-42A
D. A. Crowley, 773-43A
A. P. Fellinger, 773-41A
S. D. Fink, 773-A
K. M. Fox, 999-W
B. J. Giddings, 786-5A
N.K. Gupta, 703-41A
C. C. Herman, 999-W
C. M. Jantzen, 773-A
F. C. Johnson, 999-W
M.R. Kesterson, 703-41A
P.L. Lee, 703-41A
S. L. Marra, 773-A
D. K. Peeler, 999-W
F. M. Pennebaker, 773-42A
M. E. Stone, 999-W
D.A. Tamburello, 703-41A
W. R. Wilmarth, 773-A